Pharmacological Research 187 (2023) 106565

Contents lists available at ScienceDirect

Pharmacological Research

journal homepage: www.elsevier.com/locate/yphrs

Upgrade of chrysomycin A as a novel topoisomerase II inhibitor to curb KRAS-mutant lung adenocarcinoma progression

Junmin Zhang [a,b,1], Pei Liu [a,1], Jianwei Chen [a,c,1], Dahong Yao [a], Qing Liu [a], Juanhong Zhang [a,b,d], Hua-Wei Zhang [c], Elaine Lai-Han Leung [e,*], Xiao-Jun Yao [a,*], Liang Liu [a,*]

[a] State Key Laboratory of Quality Research in Chinese Medicine, Dr. Neher's Biophysics Laboratory for Innovative Drug Discovery, Macau University of Science and Technology, Macau
[b] School of Pharmacy, State Key Laboratory of Applied Organic Chemistry, and College of Chemistry and Chemical Engineering, Lanzhou University, Lanzhou 730000, China
[c] School of Pharmaceutical Sciences, Zhejiang University of Technology, Hangzhou 310000, China
[d] College of Life Science, Northwest Normal University, Lanzhou 730070, China
[e] Cancer Center, Faculty of Health Science, and MOE Frontiers Science Center for Precision Oncology, University of Macau, Macau

ARTICLE INFO

Keywords:
Chrysomycin A
DNA damage
Apoptosis
Topoisomerase II activity
Reactive oxygen species

ABSTRACT

A primary strategy employed in cancer therapy is the inhibition of topoisomerase II (Topo II), implicated in cell survival. However, side effects and adverse reactions restrict the utilization of Topo II inhibitors. Thus, investigations focus on the discovery of novel compounds that are capable of inhibiting the Topo II enzyme and feature safer toxicological profiles. Herein, we upgrade an old antibiotic chrysomycin A from *Streptomyces* sp. 891 as a compelling Topo II enzyme inhibitor. Our results show that chrysomycin A is a new chemical entity. Notably, chrysomycin A targets the DNA-unwinding enzyme Topo II with an efficient binding potency and a significant inhibition of intracellular enzyme levels. Intriguingly, chrysomycin A kills *KRAS*-mutant lung adenocarcinoma cells and is negligible cytotoxic to normal cells at the cellular level, thus indicating a capability of potential treatment. Furthermore, mechanism studies demonstrate that chrysomycin A inhibits the Topo II enzyme and stimulates the accumulation of reactive oxygen species, thereby inducing DNA damage-mediated cancer cell apoptosis. Importantly, chrysomycin A exhibits excellent control of cancer progression and excellent safety in tumor-bearing models. Our results provide a chemical scaffold for the synthesis of new types of Topo II inhibitors and reveal a novel target for chrysomycin A to meet its further application.

1. Introduction

Cancers are fueled by changes in DNA that tip cells towards uncontrolled multiplication. Genetic aberrations and uncontrolled cell proliferation are thus one of the hallmarks of malignant cells [1]. The overexpressing of DNA topoisomerase (Topo) as a common manifestation of both hallmarks is ubiquitous in tumor cells [2]. Topo enzymes are generally identified in two types in human cells, i.e., Topo I and Topo II. Functionally, Topo I and II enzymes catalyze and manipulate the transient breaking and rejoining of two strands of duplex DNA, e.g., cutting the phosphodiester bonds in the single-stranded and double-stranded DNA, respectively, thus altering the topology of DNA [3–5]. Especially, the Topo II enzyme has key biological functions of DNA replication, chromosome segregation and transcription, and is the second-largest chromatin protein after histones [6]. It is well recognized that the induction of apoptosis by interfering with Topo II and producing enzyme-mediated DNA damage is an effective strategy for cancer chemotherapy [7,8]. Interestingly, in the two types of Topo II enzyme, Topo IIα is upregulated during cell proliferation, while topo IIβ is equally expressed in all cells [7,9]. Thus, there is increasing attention

Abbreviations: BCA, bicinchoninic acid; DMSO, dimethyl sulfoxide; DSBs, double-strand breaks; h-Topo IIα, human Topo IIα; KRAS, Kirsten rat sarcoma viral oncogene homolog; LLC, Lewis lung carcinoma; NSCLC, non-small cell lung cancer; PARP, poly (adenosine diphosphate (ADP)-ribose) polymerase; PFA, paraformaldehyde; PI, propidium iodide; ROS, reactive oxygen species; SDS-PAGE, SDS-polyacrylamide gel electrophoresis; TOP2A, topoisomerase IIα; Topo, topoisomerase.

* Corresponding authors.
E-mail addresses: lhleung@um.edu.mo (E.L.-H. Leung), xjyao@must.edu.mo (X.-J. Yao), lliu@must.edu.mo (L. Liu).

[1] Authors are equal contributors.

https://doi.org/10.1016/j.phrs.2022.106565
Received 23 September 2022; Received in revised form 13 November 2022; Accepted 18 November 2022
Available online 19 November 2022

to the Topo IIα enzyme as an effective and selective anticancer target [10–15].

Lung cancer with a mortality rate of 18% is still the number one cause of cancer-related death worldwide [16]. Chemotherapies such as etoposide, a Topo II enzyme inhibitor with clinical benefits, effectively alleviate disease in a small number of lung cancer patients [17–19]. Thus, new Topo enzyme inhibitors or sensitizers are being considered for therapeutic intervention to benefit the continuation of this clinical event [2,20]. As part of our continued attempts to discover and develop potential small molecules from natural sources to treat non-small cell lung cancer (NSCLC) [21–27], we try to find targeted therapeutic molecules from marine-derived microbial metabolites. Since the metabolites produced by complex and diverse microorganisms are important resources for drug discovery programs [28,29]. Importantly, antibiotics with significant activity as microbial metabolites have painted a brilliant picture of antineoplastic drug development [30,31]. To this day, it is still a key area of drug development. For instance, doxorubicin, mitomycin C, and bleomycin are still important drugs for tumor chemotherapy [31].

Chrysomycins were novel antibiotic complexes isolated from *Streptomyces* and were first reported in 1955 [32]. Subsequently, several studies have reported the anti-bacteriophage and antibacterial activity of chrysomycins, such as bacterial and viral infections in purulent surgery and gynecological diseases [32,33], as well as the antitumor effect [34,35]. However, the test samples in these reports contain a mixture of analogs with unknown structures. It was not until approximately the 1980 s that chrysomycin A and B were separated and their structures were identified [35]. As a result, virenomycins and chrysomycins are re-established as the same compounds, and virenomycins are defined as a synonym for chrysomycins [36,37]. Building on these chemical efforts, chrysomycin A was subsequently confirmed to have antileukemia properties [38]. In addition, chrysomycin A has been further demonstrated to harbor a strong antifungal effect, with negligible cytotoxicity to normal cells and no effect on the lysis of red blood cells [39]. Recent studies suggest that chrysomycin A has effective anti-tuberculosis activity [39–42]. In addition, the data exhibit that chrysomycin A can reduce neuroinflammation via down-regulating the NLRP3/cleaved caspase-1 signaling pathway in lipopolysaccharide-stimulated mice and BV2 microglial cells [43]. However, the harsh separation conditions and the difficulty of total synthesis for the chrysomycin series have led to their lags in the study of the pharmacological activity [44,45]. Especially, the intracellular target(s) mediating the cytotoxic effect and antitumor mechanism have not been well defined.

The technological fermentation of chrysomycin series derived from marine-derived *Streptomyces* is the successful attempt of our efforts to obtain the lead molecules [46,47]. Fortunately, we recently isolate a sufficient amount of chrysomycin A from *Streptomyces* sp. 891 through a sophisticated technique, and further find that chrysomycin A can significantly ablate NSCLC in the Kirsten rat sarcoma viral oncogene homolog (KRAS) mutation cell lines and the Lewis lung carcinoma implantation model. The follow-up studies demonstrate that chrysomycin A pronouncedly inhibits the activity of Topo II enzyme and triggers the accumulation of reactive oxygen species (ROS), thereby inducing DNA damage-mediated apoptosis of KRAS mutant cells NCI-H358. Our results are the first to systematically present chrysomycin A as a new Topo II enzyme inhibitor in the treatment of solid tumors, and provide a basis for the further development of chrysomycin A as an anticancer candidate.

2. Materials and methods

2.1. Chemistry

2.1.1. Strain materials and optimal fermentation conditions

The marine strain *Streptomyces* sp. 891 is derived from the mangrove sediments in the South China Sea. The optimal fermentation conditions for chrysomycin A are as follows [46]: i) the medium consists of 40 g/l glucose, 25 g/l hot-pressed soybean meal, 20 g/l corn starch, 3 g/l $CaCO_3$; ii) by orthogonal experiments and single-factor at shaking flask level, the fermentation time was 168 h, the seeding age was 48 h, the initial pH was 6.5, the carrier liquid volume was 30 ml, the inoculum volume was 5.0%, and the shaking speed was 220 rpm.

2.1.2. Chemical characterization and purity analysis

The structure of chrysomycin A was characterized by ^{1}H and ^{13}C NMR, as well as ESI-MS (Table S1 and Fig. S1-S3) [40], and the purity was identified by HPLC (purity >98%, Fig. S4). The analysis was performed on HPLC at room temperature. Chrysomycin A was dissolved in chromatographic methanol. The injection volume was 10 μl. The mobile phases were acetonitrile and water (1:1), and the flow rate is 1.0 ml/min. The maximum absorbance is used as the detection wavelength at 254 nm.

2.2. Cell culture and reagents

NSCLC cell lines with *KRAS* mutations, NCI-H358, NCI-H2122, and NCI-H23 cells, as well as a human normal lung epithelial cell line, BEAS-2B cells, were purchased from the ATCC. All cell lines used in this study were cultured at 37 °C with 5% CO_2 in RPMI 1640 or DMEM medium supplemented with 10% fetal bovine serum (FBS), 4 mM L-glutamine, and penicillin/streptomycin according to the manufacturer's instructions.

RPMI 1640, DMEM medium, and antibiotics were supplied by Lonza (NJ, USA). Dimethyl sulfoxide (DMSO) and MTT reagent were obtained from Acros Organics (NJ, USA). Topo II enzyme drug screening kit was obtained from TopoGEN (CO, USA). Annexin V-FITC/propidium iodide (PI) staining kit was obtained from BD Biosciences (CA, USA). H_2DCFDA was obtained from TargetMol (MA, USA). FBS was purchased from Gibco (CA, USA). The primary antibodies against PARP, cleaved caspase-3, cleaved PARP, and GAPDH were purchased from Cell Signaling Technology (MA, USA). The primary antibody topoisomerase IIα (TOP2A) was obtained from OriGene (MD, USA). The anti-γ-H2AX was obtained from FineTest (Wuhan, China). The anti-mouse secondary antibodies, anti-rabbit secondary antibodies, and fluorescein-conjugated goat anti-rabbit antibody were obtained from Odyssey (ME, USA). Fluorescein-conjugated mouse antibody and Trizol reagent were obtained from Invitrogen (CA, USA). Cisplatin (purity ≥ 99.0%) was purchased from Sigma (MO, USA). Chrysomycin A was dissolved in DMSO to prepare a 10 mM stock solution and experimental dilutions for cell culture were prepared in RPMI 1640/10% FBS. All other reagents were of analytical grade.

2.3. Viability assays

Viability was evaluated by the MTT assay [26]. NCI-H358, NCI-H2122, NCI-H23 cells, and BEAS-2B cells were dissociated, counted and plated in 96-well microplates (Falcon) with 5000 cells per well and allowed to adhere overnight. Subsequently, these cells were added with increasing concentrations of chrysomycin A or vehicle (0.1% DMSO final) for 48 h unless otherwise noted. Edge wells were filled with PBS. At the end of the treatment10 μl of MTT reagent (5 mg/ml) was added to each well and incubated at 37 °C for an additional 4 h. Then, the reagent was removed and 100 μl DMSO was added. After incubation with gentle agitation for 10 min, the viability was calculated by measuring absorbance at 570 nm and 650 nm using a microplate reader (Tecan, Morrisville, NC, USA).

2.4. Molecular docking

Schrödinger molecular modeling software (Schrödinger, LLC, New York, NY, USA, Release 2015) was employed for molecular docking research (Schrödinger, version 10.1; Schrödinger, LLC: New York, 2015)

[48,49]. The 2D structure of the ligand was converted into a full 3D structure by distributing the OPLS-2005 force field, and the ligand was prepared by the *LigPrep* 3.3 module in Schrödinger 2015. The ionized states, stereoisomers, and tautomers of the ligand were predicted by using the Epik module at a pH 7.0 ± 3.0 implemented in Schrödinger. The crystal structure of the human Topo IIα enzyme complexed with known inhibitors, etoposide, was extracted from the protein database (PDB ID: 5GWK), and then prepared with the Protein Preparation Wizard in Schrödinger. During the protein preparation process, all heteroatoms and water molecules were removed. Hydrogen atoms were added, and the active sites of the protein were defined to create a grid. The size of the grid box at the active site is limited to 20 Å. Subsequently, chrysomycin A was docked to the binding site of the human Topo IIα enzyme by using the Glide-program with standard extra precision [48,49]. The combination of chrysomycin A and Topo IIα enzyme adopts more than one conformation, emphasizing the importance of the lowest energy conformer of chrysomycin A for docking research. The best binding pose for chrysomycin A with the human Topo IIα enzyme was preserved.

2.5. DNA Topo IIα enzyme inhibitory activities analysis in vitro

The inhibitory activities of the positive drug etoposide and chrysomycin A on DNA Topo IIα enzyme were measured by the DNA Topo IIα drug screening kit (TopoGEN, Columbus, Ohio, USA) according to the manufacturer's instructions, and observed by Topo IIα-mediated DNA cleavage analysis [50]. Briefly, the reaction mixture (final volume 20 μl) contains PBR322 plasmid DNA (0.65 μg), 50 mM Tris-HCl (pH 8.0), 10 mM $MgCl_2$, 150 mM NaCl, 5 mM dithiothreitol, 30 μg/ml BSA, specified drug concentration (1% DMSO) and 0.75 unit Topo IIα. The reaction mixture was incubated at 37 °C for 30 min, and the reaction was stopped by adding 2 μl of 10% SDS. Then 2 μl 10 × gel loading buffer (0.25% bromophenol blue, 50% glycerol) was added to the system. The reaction product was electrophoresed on a 0.8% agarose gel with TAE (tri-acetate-EDTA) running buffer at 50 V for 1 h. After the gel was stained with ethidium bromide (0.5 μg/ml) for 60 min, the DNA bands were visualized under ultraviolet light and scanned with the LI-COR Odyssey Scanner.

2.6. Assay of intracellular Topo II enzyme levels

The Topo II α (*TOP2A*) gene encodes the DNA Topo II enzyme. The activity of Topo II enzyme in the NCI-H358 cells was evaluated by detecting the protein expression of TOP2A [51,52]. NCI-H358 cells were treated with different concentrations of chrysomycin A for 24 h and then processed to obtain protein samples. An equal amount of cell lysate (5 μg per lane) was separated by SDS-polyacrylamide gel electrophoresis (SDS-PAGE) and immunoblotted with anti-*TOP2A*.

2.7. Assay of intracellular γ-H2AX levels

The intracellular γ-H2AX levels were analyzed by western blot as a biomarker reflecting DNA double-strand damage. NCI-H358 cells were treated with different concentrations of chrysomycin A for 24 h and then processed to obtain protein samples. An equal amount of cell lysate (10 μg per lane) was separated by SDS-PAGE and immunoblotted with anti-*γ-H2AX* [53].

2.8. Western blot analysis

After treating NCI-H358 cells with the indicated concentration of chrysomycin A for 24 h, the cells were harvested and lysed repeatedly on ice in RIPA lysis buffer containing protease and phosphatase inhibitors for 30 min. The lysates were centrifuged at 12,000 rpm for 15 min at 4 °C, and the protein concentration in the supernatant was determined with the bicinchoninic acid (BCA) protein assay kit. After preparing the protein sample, SDS-PAGE loaded and separated the same amount of protein. Subsequently, the protein was electro-transferred to the PVDF membrane, blocked with 5% skimmed milk in TBST buffer (0.1% Tween 20 in TBS) at room temperature for 2 h, and then washed with 1 ×TBST for 3 times. The membrane was incubated with the corresponding stock solution with antibodies against specific proteins at 4 °C overnight. The blot was washed and incubated with the secondary antibody solution for 2 h at room temperature. The bands were visualized using the Pierce ECL Western Blotting Kit or LI-COR Odyssey scanner [26,54].

2.9. ROS assay

H_2DCFDA staining was performed to detect the level of ROS in cells. NCI-H358 cells (2×10^5) were seeded on a 6-well plate and treated with different concentrations of chrysomycin A for 6 h, and then incubated with pre-warmed 1 μM H_2DCFDA in PBS for 30 min at 37 °C [25,55]. The cell samples were collected and suspended in PBS. The analysis was performed on the BD Aria III flow cytometer. The FlowJo software v10 was assayed for results.

2.10. Colony formation assay

NCI-H358 cells were seeded into a 6-well plate with 2000 cells per well and cultured overnight for attachment. The cells were exposed to different concentrations (0, 0.0075, 0.015, 0.03, and 0.06 μM) of chrysomycin A for 14 days. The culture medium was changed every 72 h with medium with or without chrysomycin A. When colony formation was visible, the medium was drained. The colonies were washed with cold PBS, and were fixed with 4% paraformaldehyde (PFA) for at least 30 min. Finally, the colonies were stained with 0.2% crystal violet solution in 10% ethanol for 20 min to visualize [26].

2.11. Apoptosis assay

Apoptotic cells were assayed for Annexin V-FITC/PI staining kit (BD Biosciences) [27,56]. NCI-H358 cells were plated in a 6-well plate at a confluence of 50%. After 24 h, the cells were treated with chrysomycin A at the specified concentration for 24 h. Subsequently, the cells were washed at least twice with 1 ×PBS, trypsinized, and resuspended in 100 ml Annexin V binding buffer. Finally, the cells were stained with Annexin V-FITC and PI and incubated in the dark for 15 min, and then analyzed and collected data on a BD Aria III flow cytometer. At least 10,000 cells were measured for each sample. The results are expressed as Annexin V-FITC/PI unstained cells of untreated (DMSO) versus chrysomycin A treated samples, and analyzed by FlowJo software v10.

2.12. Cell cycle analysis

Cell cycle analysis was performed by flow cytometry [27]. The cells laid in the 6-well plate were treated with chrysomycin A for 24 h according to the instructions. The cells were then trypsinized, collected (including unattached cells), and washed with PBS. The cell pellets were resuspended in 70% ethanol at 4 °C for at least 30 min. After fixation, the cells were centrifuged at 1000 rpm for 5 min to remove ethanol. Each cell pellet was resuspended in 500 μl PI staining solution at 37 °C in the dark for 30 min and then washed twice in PBS. The cells were resuspended in 300 μl 1 ×binding buffer and transferred to a BD Aria III flow cytometer for analysis. The indicated population was quantified by using FlowJo software V10.

2.13. Xenograft assay

All mice were bred in the State Key Laboratory of Quality Research in Chinese Medicine, and all animal experiments were conducted following relevant guidelines and regulations approved by the Institutional Animal Care and Use Committee. Lewis lung carcinoma cells (1×10^6) in

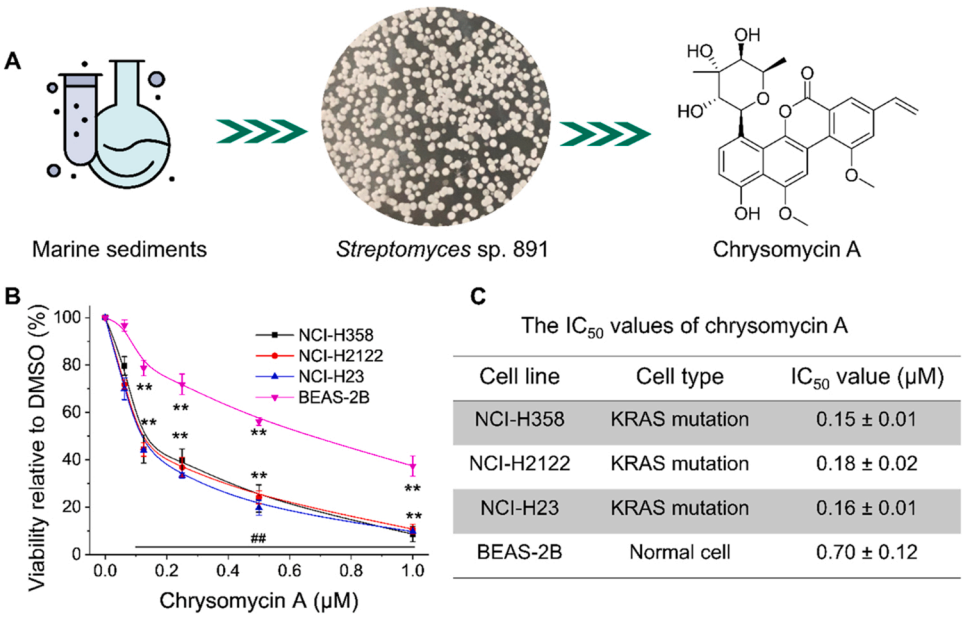

C

The IC_{50} values of chrysomycin A

Cell line	Cell type	IC_{50} value (μM)
NCI-H358	KRAS mutation	0.15 ± 0.01
NCI-H2122	KRAS mutation	0.18 ± 0.02
NCI-H23	KRAS mutation	0.16 ± 0.01
BEAS-2B	Normal cell	0.70 ± 0.12

Fig. 1. Chrysomycin A produced by marine-derived *Streptomyces* sp. 891 acts on non-small cell lung cancer (NSCLC) cells with *KRAS* mutation. (A) Chrysomycin A derived from a strain of *Streptomyces* sp. 891 in marine sediments. (B) Selective cytotoxicity of chrysomycin A. (C) The IC_{50} values of cell viability from chrysomycin A. NSCLC cells NCI-H358, NCI-H2122, and NCI-H23 with *KRAS* mutations, as well as normal lung epithelial cells BEAS-2B were treated with different concentrations of chrysomycin A for 48 h. The cell survival rate was measured by the MTT method, and the inhibition rate is expressed as a percentage relative to the effect of DMSO. Data in B are from three independent experiments done in triplicate, and the results are expressed as the mean ± SD, $^{**}p < 0.05$ versus the control groups, $^{\#\#}p < 0.05$ versus the BEAS-2B cells.

120 μl FBS-free medium were mixed with 80 μl Matrigel with reduced growth factors and then injected subcutaneously into the right side of 6-week-old C57BL/6 mice. After the xenograft reached approximately 80 mm^3, the C57BL/6 mice were randomly divided into four experimental groups and administered intraperitoneally with the vehicle (2% DMSO, 40% PEG400, and 5% Tween-80 in normal saline), cisplatin (2 mg/kg, *i.p.*), or chrysomycin A (10, or 20 mg/kg, 40% PEG400 and 5% Tween-80 in normal saline) once a day for 15 days. The body weight and tumor size of the mice were measured every 3 days to evaluate tumor growth. The tumor volume was calculated as length (mm) × width (mm) $2 \times \pi/6$. The mice were sacrificed at the end of the experiment and the tumor tissues and organs were removed for further analysis [24,27].

2.14. Statistical analysis

All quantitative data were expressed as the mean ± SD of at least three independent experiments. Comparisons among multiple groups were performed using a one-way analysis of variance (ANOVA) followed by a post hoc Scheffe test. Statistical differences between the two groups were assessed by the Student's t-test. Values of less than 0.05 were considered significant. Statistical analysis and IC_{50} value were carried out using GraphPad Prism 8.

3. Results

3.1. Obtaining of high-purity and considerable-yield chrysomycin A

Chrysomycin A in this work was isolated from marine sediments-derived strain *Streptomyces* sp. 891 [46] (Fig. 1 A). The structure of chrysomycin A was characterized by ^{1}H and ^{13}C NMR, as well as ESI-MS (Table S1 and Fig. S1-S3) [40], and the purity was identified by HPLC (purity >98%, Fig. S4). In recent years, marine sediments have received widespread attention in providing effective strains [57]. As described in the preparation process in the materials and methods, we established the optimal fermentation conditions and medium composition for the efficient production of chrysomycin A, and obtained high-purity and considerable-yield chrysomycin A, providing a material basis for our follow-up pharmacological activity research.

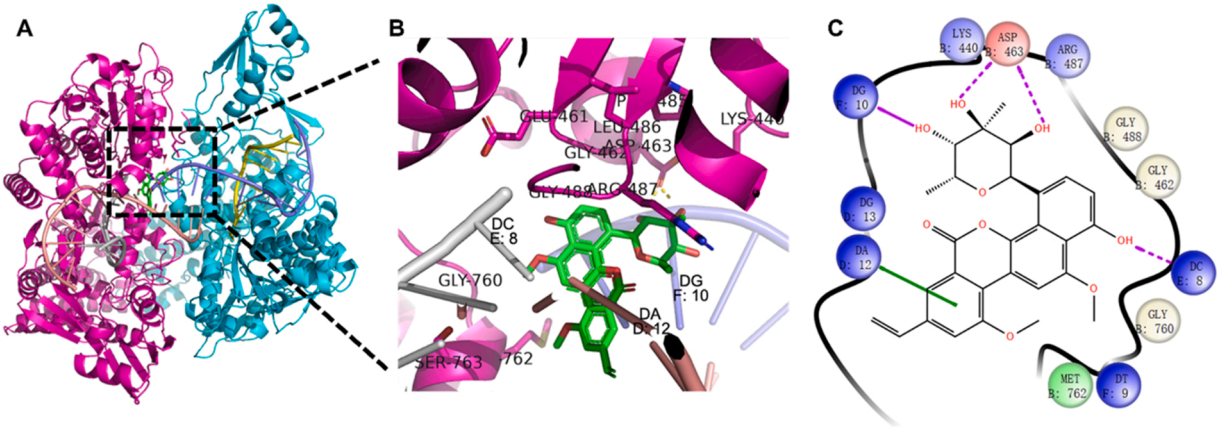

Fig. 2. Chrysomycin A targeting Topo II enzyme by molecular docking. (A) Schematic diagram of Topo II docking analysis. The 3D molecular docking of chrysomycin A on the crystal structure of human Topo IIα (PDB ID: 5GWK) by using Schrödinger molecular modeling software (Schrödinger, LLC, New York, NY, USA, Release 2015). (B) Enlarged schematic diagram of chrysomycin A in complex with the active site residues of DNA Topo II enzyme and DNA bases. Etoposide was used to indicate the Topo II binding site of DNA in the docking. (C) Docked position of chrysomycin A. Chrysomycin A revealed the pi-pi stacking with base DA12, as well as the H-bonds with ASP 463, DC8, or DG10.

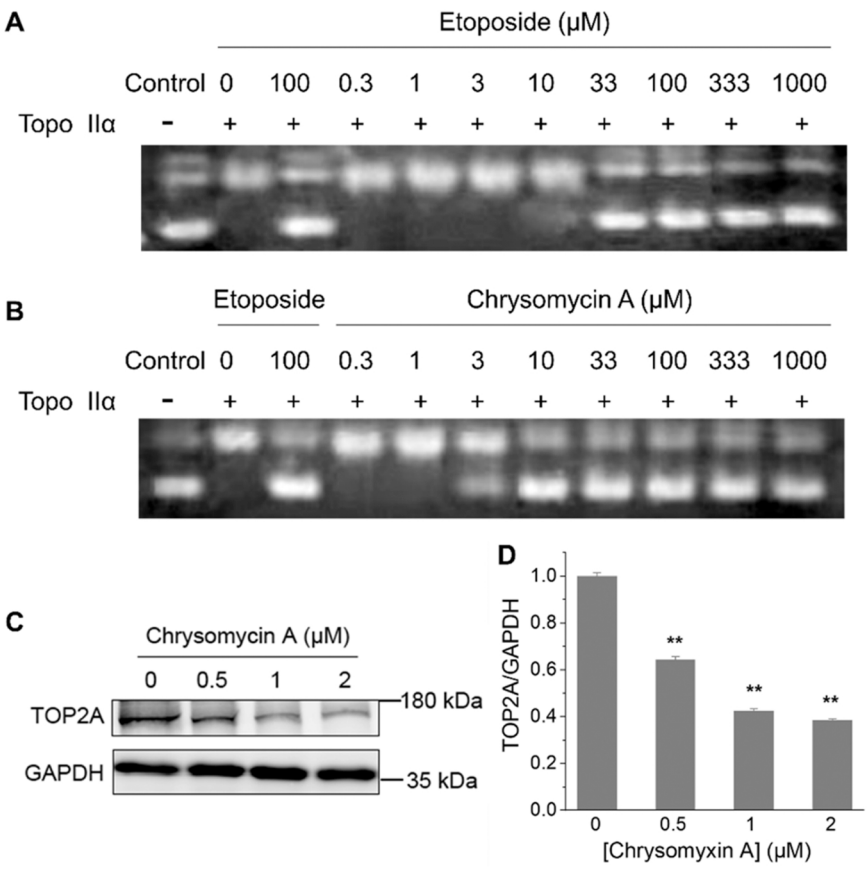

Fig. 3. Inhibition of Topo II enzyme by chrysomycin A. (A) The inhibitory activity of etoposide on pure human Topo II α enzyme. (B) The inhibitory activity of chrysomycin A on pure human Topo II α enzyme. The inhibitory activity was evaluated by in vitro biochemical analysis. Different doses of chrysomycin A or etoposide and Topo II α were evaluated for DNA relaxation by 1% agarose gel electrophoresis in the presence of ethidium bromide. The control group only had pBR322 DNA, while the drug group was treated with the concentration shown in the figure in the presence of pBR322 DNA and Topo II α. (C) Downregulation of TOP2A in NCI-H358 cells by chrysomycin A. (D) The protein band was quantified from (C) by ImageJ. The specified concentration of chrysomycin A was treated with NCI-H358 cells for 24 h. The cells were collected and lysed, and then the protein was quantified. The expression of Topo II enzyme (TOP2A) in the protein was detected by western bolts. The results are expressed as the mean ± SD, and * * $p < 0.05$ versus the control group in (D).

3.2. Cytotoxicity of chrysomycin A toward NSCLC cells with KRAS mutations

In our attempt to explore and discover bioactive molecules for the treatment of NSCLC with KRAS mutation [26,54,58], the cytotoxicity of chrysomycin A was initially conducted with three NSCLC cell lines with KRAS mutation, NCI-H358, NCI-H2122, and NCI-H23 cells, respectively, as well as BEAS-2B cells, a human normal lung epithelial cell line. Interestingly, chrysomycin A significantly ablated NCI-H358, NCI-H2122, and NCI-H23 cells in a dose-dependent manner, and the IC_{50} values of cell survival rates at 48 h were 0.15 ± 0.01 μM, 0.18 ± 0.02 μM and 0.16 ± 0.01 μM, respectively (Fig. 1B and C). Meanwhile, chrysomycin A also exhibited definite cytotoxicity to BEAS-2B cells under the same experimental conditions (Fig. 1B), and the IC_{50} value of cell survival rate at 48 h was 0.70 ± 0.12 μM. Intriguingly, the cytotoxic effect of chrysomycin A in KRAS mutation NCI-H358 cells was approximately five-fold compared with that in normal lung epithelial BEAS-2B cells. This friendly security in a certain drug concentration range is also consistent with recent literature [39]. The results indicate that chrysomycin A is cytotoxic to NSCLC with KRAS mutation and relatively safe to normal cells under our experimental conditions.

3.3. Chrysomycin A targeting Topo II enzyme by molecular docking

Given the excellent intracellular potency and selectivity of chrysomycin A, further interrogating its action mechanism should be on the agenda. Considering the following points, i.e., i) the naphthocoumarin glycoside antibiotics, such as gilvocarcin V, were reported to bind to or intercalate with DNA to interfere with the repair of damaged DNA [59]. In terms of structure, chrysomycin A also belongs to this class of antibiotics [38]; ii) chrysomycin A is similar in planar structure to etoposide (a robust Topo II enzyme inhibitor), especially both contain functional groups that can form pi-pi stacking and hydrogen bonds with Topo II enzyme or DNA bases [60,61]. Thus, we simulated the 3D molecular docking of chrysomycin A on the crystal structure of human Topo IIα (h-Topo IIα, PDB ID: 5GWK) by using Schrödinger molecular modeling software (Schrödinger, LLC, New York, NY, USA, Release 2015) [48,49]. The binding energy of chrysomycin A with the Topo II enzyme and its mode of interaction with the active site of the enzyme has been evaluated for the first time (Fig. 2 A, B, and C). We used the hydrogen bonds and pi interactions between chrysomycin A and surrounding amino acids and sliding scores to predict the binding affinity and optimal arrangement of chrysomycin A at the active site of the Topo II enzyme. As the results shown in Fig. 2 A and B, the schematic diagram indicated that chrysomycin A is inserted into the recognition site of DNA via the Topo II enzyme. Briefly, chrysomycin A exhibited a potent interaction between ASP 463, one of the important active site residues of DNA Topo II enzyme, and DNA bases (Fig. 2B). The docking position of chrysomycin A showed the pi-pi stacking with base DA12, as well as the H-bonds with ASP 463, DC8 or DG10 (Fig. 2 C). Moreover, the established docking program was also verified by etoposide. The docking score of Topo II enzyme with chrysomycin A was similar to that of etoposide, being − 8.87 and − 8.94 respectively [53]. Importantly, this binding mode is also consistent with the currently reported binding pattern of several Topo II enzyme poisons, i.e., focusing on DNA Topo II enzyme active residues and DNA bases [53,61,62]. These results suggest that chrysomycin A has a robust binding ability with the DNA Topo II enzyme.

3.4. Proof of chrysomycin A targeting Topo II enzyme by inhibiting enzyme activity

To evaluate the inhibitory effect of chrysomycin A on the activity of pure DNA Topo II enzyme, the inhibition of h-Topo II enzyme from the

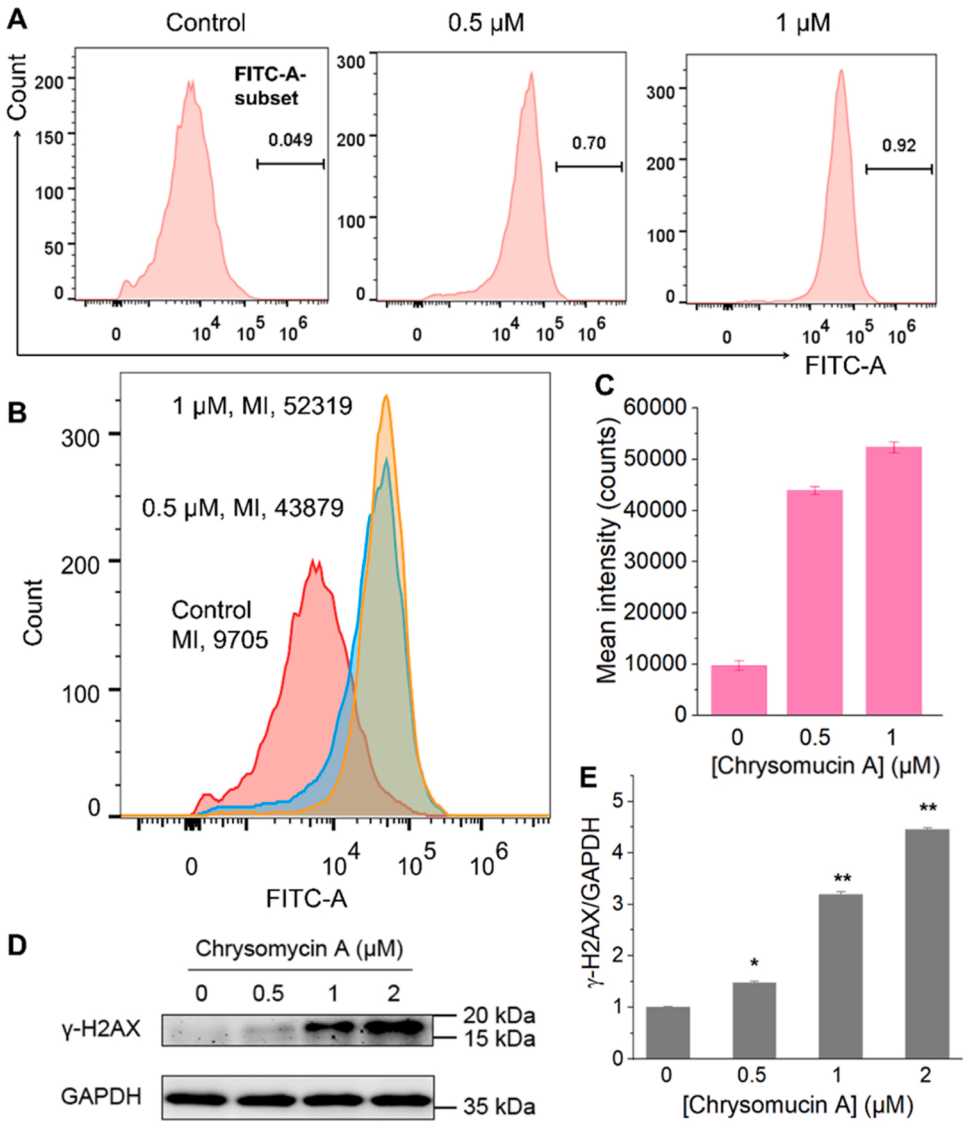

Fig. 4. Induction of ROS accumulation and DNA damage. (A) Accumulation of ROS triggered by chrysomycin A. NCI-H358 cells treated with the specified concentration of chrysomycin A (0, 0.5, or 1 μM) for 6 h were incubated with the ROS indicator H2DCFDA to detect endogenous ROS by flow cytometry. (B and C) Statistical results of A were displayed quantitatively with a histogram. (D) Up-regulation of γ-H2AX expression levels triggered by chrysomycin A. Expression levels of γ-H2AX protein were detected by western blots after treatment with chrysomycin A (0, 0.5, 1, or 2 μM) for 24 h. (E) Relative protein level was quantified by densitometry using ImageJ. The results are expressed as the mean ± SD, and * * $p < 0.05$ versus the control group in (E).

conversion of supercoiled pBR322 plasmid DNA by chrysomycin A was then monitored using a relaxation assay [50]. As described in materials and methods, DNA relaxation was assessed by 1% agarose gel electrophoresis in the presence of ethidium bromide. The etoposide was applied as a positive control. The effect of chrysomycin A on the h-Topo II enzyme showed an inspiring inhibitory effect. Under our experimental conditions, chrysomycin A exhibited a slightly better result than the positive drug etoposide (Fig. 3 A and B). Notably, the classic Topo II-mediated cleavage assay and the DNA unwinding assay can also further elucidate the mechanism of chrysomacin A in vitro [63,64]. In addition, the Topo II enzyme activity of NCI-H358 cells treated by chrysomycin A was tested [65]. The Topo IIα (*TOP2A*) gene encodes the DNA topoisomerase. Equivalent amounts of cell lysates (5 μg per lane) were thus separated by SDS-PAGE and immunoblotted with anti-*TOP2A*. The results indicated that chrysomycin A inhibits the Topo II enzyme activity in NCI-H358 cells in a dose-dependent manner (Fig. 3 C and D), suggesting that the expression of *TOP2A* in cells is down-regulated after continuous drug treatment. Differences in experimental concentrations were observed due to factors such as the sensitivity of the pure enzyme and intracellular Topo IIα assays. Nonetheless, this observation is also present in the positive drug etoposide reported in the literature [50]. In aggregate, these results, together with docking simulations, indicate that chrysomycin A inhibits Topo II enzyme activity and interacts with DNA.

3.5. Induction of ROS accumulation and DNA damage by chrysomycin A

Since chrysomycin A targets the DNA Topo II enzyme and reduces especially the expression of Topo II enzyme in NCI-H358 cells. Chrysomycin A treatment may thus induce further intracellular DNA damage. In evaluating the cellular DNA damage treated by chrysomycin A, we first tested the accumulation of intracellular ROS that also triggers the DNA damage in NCI-H358 cells. The early administration of chrysomycin A causes a large amount of ROS production in cells [38], together with the further reduction of Topo II enzyme activity, both will thus inevitably lead to increased cellular DNA damage. As we expected, 0.5 and 1 μM chrysomycin A was administered to NCI-H358 cells for 6 h, which dramatically stimulated the accumulation of ROS in NCI-H358 cells (Fig. 4 A and B). Fig. 4 C is a quantitative representation of the fluorescence results. After accumulating this evidence, we then evaluated the DNA damage in NCI-H358 cells treated with chrysomycin A. Given that the phosphorylation of serine 139 of H2AX is a broadly used biomarker reflecting DNA double-strand damage, our results are also indicated by the up-regulation of γ-*H2AX* expression levels. In our results, the γH2AX protein expression was upregulated noticeably in a concentration-dependent manner after 24 h of treatment with 0.5, 1, 2 μM chrysomycin A in NCI-H358 cells (Fig. 4D), suggesting that chrysomycin A causes DNA damage in NCI-H358 cells. The

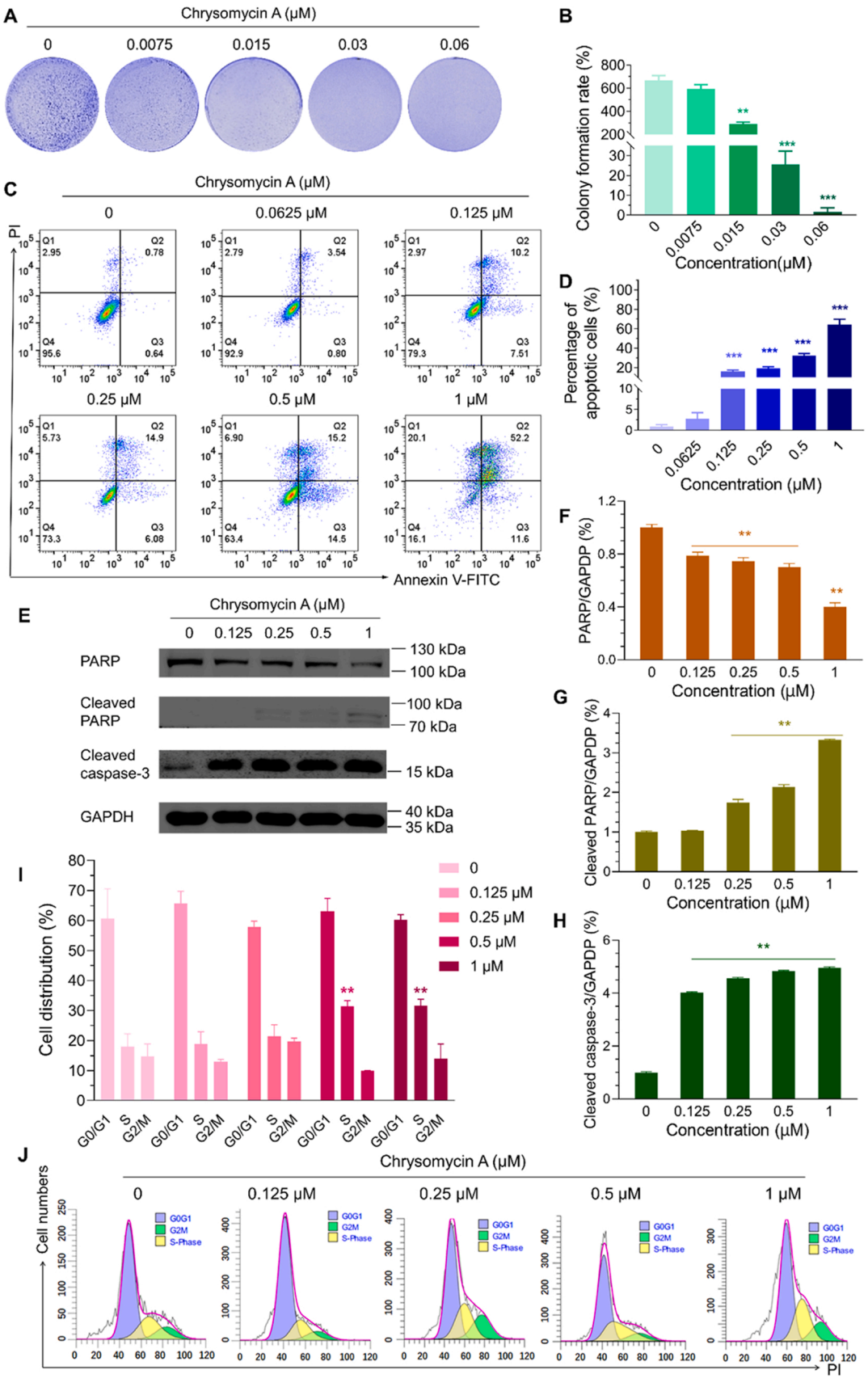

(caption on next page)

Fig. 5. Effect of chrysomycin A on the proliferation of NCI-H358 cells. (A) Dose-dependent effect of chrysomycin A on colony formation of NCI-H358 cells. (B) Statistical results of the A indicate that chrysomycin A suppressed the colony-forming ability of NCI-H358 cells after treating NCI-H358 cells with indicated concentrations for 14 days. (C) Induction of NCI-H358 cell apoptosis through counting by the flow cytometry. NCI-H358 cells were incubated with the indicated concentrations of chrysomycin A for 24 h and stained with Annexin V-FITC and propidium iodide (PI). (D) Columns show the percentage of apoptosis cells. (E) Western blot analysis was performed with antibodies specific for PARP, cleaved PARP, and cleaved caspase-3, and GAPDH as the loading control. NCI-H358 cells were treated with indicated concentrations of chrysomycin A for 24 h and lysed, and the protein was extracted. (F) Statistical results of the E show that the chrysomycin A treatment down-regulated the expression level of PARP protein. While the quantitative analysis of the E indicates that the chrysomycin A treatment up-regulated cleaved PARP and cleaved caspase 3, which are represented in (G) and (H), respectively. (I) Columns showing the percentage of NCI-H358 cells in the G0/G1, S, and G2/M phases of the cell cycle suggest that the cell cycle was accumulated at the S phase begun at the treatment of 0.5 μM chrysomycin A. (J) The distribution of the cell cycle was monitored by flow cytometry. NCI-H358 cells were treated with the indicated concentrations of chrysomycin A for 24 h and then stained for analysis. The results are expressed as the mean ± SD, and * *$p < 0.01$, * **$p < 0.001$ versus the control groups.

quantification of protein expression is shown in Fig. 4E. Collectively, these results confirm that the accumulation of ROS triggered by chrysomycin A, together with the reduction of Topo II enzyme activity caused by chrysomycin A, induces intracellular DNA damage.

3.6. Inhibiting the proliferation of NCI-H358 cells by apoptosis and cell cycle arrest

Chrysomycin A strikingly induces ROS accumulation and DNA damage in cells. The occurrence of both cellular events can suppress cell proliferation [66,67]. Thus, we evaluated the effect of chrysomycin A on the proliferation of NCI-H358 cells in multiple ways. First, the results of the clonogenic growth of NCI-H358 cells by chrysomycin A stated that chrysomycin A robustly suppresses the colony-forming ability of NCI-H358 cells in a dose-dependent way after treating NCI-H358 cells with different concentrations of chrysomycin A for 72 h (Fig. 5 A and B), indicating that chrysomycin A pronouncedly inhibit the proliferation of NCI-H358 cells. Then, we performed double staining reagents, i.e. Annexin V-FITC and PI, to examine whether chrysomycin A triggers apoptosis in NCI-H358 cells through counting by the flow cytometry. As expected, the results showed that the percentages of apoptotic cells compared with the control group were 2.8%, 15.9%, 19.4%, 32.3% and 64.2% respectively after treatment of NCI-H358 cells with 0.0625, 0.125, 0.25 0.5, and 1 μM chrysomycin A for 24 h (Fig. 5 C and D). To further substantiate the apoptosis-inducing effect of chrysomycin A, we estimated the levels of pro-apoptotic factors. Cleaved-poly (adenosine diphosphate-ribose) polymerase (PARP) is considered to be an important indicator of cell apoptosis and is ordinarily considered to be an indicator of caspase 3 activation [68]. We found that the levels of cleaved-PARP and cleaved-caspase 3 were highly increased after 24 h of chrysomycin A treatment (Fig. 5E, G and H); while the levels of full-length PARP were reduced by chrysomycin A in a dose-dependent fashion (Fig. 5E and F). These results suggest that chrysomycin A promotes apoptosis of NCI-H358 cells. Antitumor antibiotics as non-specific drugs for the cell cycle generally act in the cell S phase progression. Thus, we examined the cell cycle distribution of NCI-H358 cells after chrysomycin A treatment. As shown in Fig. 2I and J, chrysomycin A continued to act on NCI-H358 cells at concentrations of 0.125, 0.25, 0.5, and 1 μM for 24 h, and the minimum dose required to induce cell S phase arrest was 0.5 μM, indicating that the inhibitory effect of chrysomycin A on cell proliferation is achieved through cell cycle arrest. Together, these key results indicate that chrysomycin A suppresses the proliferation of NCI-H358 cells by apoptosis and cell cycle arrest.

3.7. Curbing the progression of lung tumor growth in vivo

Given that chrysomycin A prominently inhibits the proliferation activity of KRAS mutant cell lines, we further evaluated its antitumor activity in the *vivo* xenograft model. According to current knowledge, the observation that chrysomycin A curbs tumor growth in *vivo* is presented here for the first time. We established an animal model of lung cancer by subcutaneously injecting Lewis lung carcinoma (LLC) cells into C57BL/6 mice. Seven days after LLC cells were implanted, the transplanted tumor volume reached approximately 80 mm^3. Subsequently, both concentrations (10, or 20 mg/kg) of chrysomycin A were conducted with treating the mice. Meanwhile, a single dose of cisplatin (2 mg/kg, *i.p.*) was also administered as a positive control. Interestingly, chrysomycin A treatment prolonged the survival time of the mice (Fig. 6 A). The bodyweight of mice and tumor size were recorded every 3 days. The results displayed that the survival rate of tumor-bearing LLC mice treated with chrysomycin A was improved (Fig. 6B). Importantly, compared with the untreated group, the bodyweight of mice treated with chrysomycin A has not changed (Fig. 6 C), and the 10 mg/kg chrysomycin A treatment suppressed the tumor growth of LLC mice from the 12th day (Fig. 6D). Especially the results of tumor volume showed an inhibitory effect from the 12th day to the 15th day (Fig. 6D), and the tumor weight of LLC mice treated with chrysomycin A was prominently lower than that of the control group (Fig. 6E). Organ indexes were tested as an assessment factor for detecting the toxicity of antitumor drugs to organs. Our statistical results showed that there are no significant differences in organ (heart, spleen, lung, kidney, thymus, and liver) indexes between the treatment group and the vehicle group (Fig. 6 F), indicating that chrysomycin A has no remarkable toxic effect on the important organs of the mice. These results evaluated the anti-lung cancer effect of chrysomycin A in vivo, proving that chrysomycin A has robustly promising therapeutic potential.

4. Discussion

KRAS is one of the most frequently mutated oncogenes in lung cancer. The development of effective pan-molecules targeted therapy is the fundamental strategy for the treatment of *KRAS*-mutant cancers [21,69]. Small molecules targeting Topo enzymes as a classic cancer treatment strategy have made outstanding contributions to the field, and this research passion is still in progress [2,70]. The discovery of new high-potency Topo II enzyme inhibitors and perfect Topo II inhibitor sensitizers, as well as a reasonably designed combination of Topo II enzyme inhibitors, are continued powerful therapeutic strategies [2, 17–20,71]. For instance, multiple etoposide combination therapies are still undergoing clinical trials in full swing [17–19]. Importantly, the recently revealed cryo-EM structures of the entire human Topo IIα nucleoprotein complex in different conformations provide a structural basis for allosteric regulation of human Topo IIα enzymes and reveals that the C-terminal domain plays a pivotal role in the regulation of enzyme activity [72]. The binding patterns in these structures provide a reference for the discovery of novel Topo II inhibitors. Together, the discovery of new chemical entities of Topo enzyme inhibitors will undoubtedly provide a material basis for this strategy, and will also provide suggestions for cancer therapy.

Although chrysomycin A was discovered earlier, its pharmacological activity especially its antitumor mechanism is lacking due to the relative difficulties of chemical separation and total synthesis [44,45]. Note that in recent years, the total chemical synthesis and biosynthesis of chrysomycin compounds have attracted attention [45,73], thus the in-depth exploration of their activities will also usher in opportunities. As a paradigm, we present here the isolated chrysomycin A as a new entity of Topo II enzyme inhibitor, which curbs *KRAS*-mutant lung

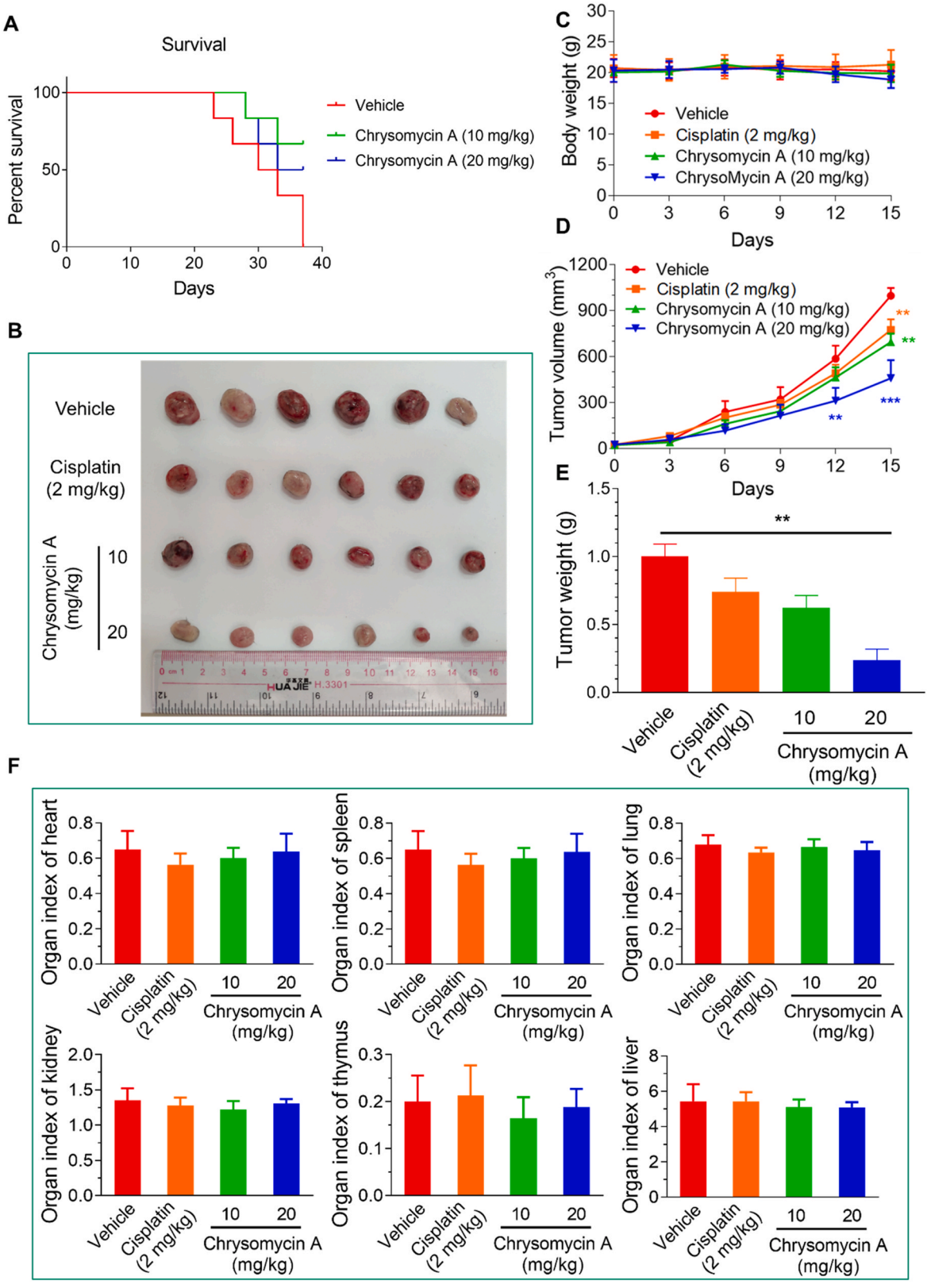

Fig. 6. Repressing the progression of lung tumor growth in the *vivo* xenograft model. (A) Examination of the effect of chrysomycin A on the survival rate of mice. (B) Representative tumor images of tumor-bearing mice after 15 days of treatment with chrysomycin A, cisplatin, and vehicle. (C) Trends of weight change of mice. (D) Trends of tumor volume were calculated every 3 days after treatment with chrysomycin A, cisplatin, and vehicle. (E) Tumor weight after the treatment ended in the treatment group and the vehicle group. (F) Organ (heart, spleen, lung, kidney, thymus, and liver) indexes after treatment with chrysomycin A, cisplatin, and vehicle. The results are expressed as the mean ± SD, and * *p < 0.01, * **p < 0.001 versus the vehicle groups in (D) and (E).

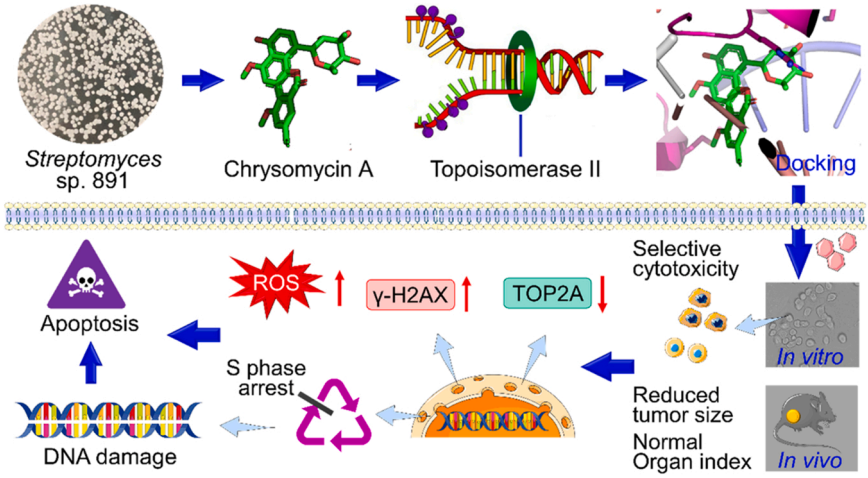

Fig. 7. Revealing an old antibiotic chrysomycin A from *Streptomyces* sp. 891 for targeting Topo II enzyme to induce DNA damage-mediated apoptosis and curb KRAS-mutant lung adenocarcinoma progression.

adenocarcinoma progression by targeting Topo II enzyme and stimulating ROS accumulation to induce DNA damage-mediated apoptosis in NCI-H358 cells (Fig. 7). Interestingly, the latest research demonstrates that chrysomycin A plays an important role in inhibiting the Topo I of *Mycobacterium tuberculosis* [42]. Human Topo I and bacterial Topo I are similar in structure to some extent, chrysomacin A may thus be a dual inhibitor of Topo I/II, which is worth further exploring.

One of the cardinal goals of clinical oncology has been to develop therapies that promote the effective elimination of cancer cells through apoptosis [68]. The triggering of cancer cell apoptosis by DNA damage is a key signal pathway for drugs to induce cell apoptosis [68]. Our results indicated that chrysomycin A binds to DNA Topo II enzymes and DNA bases effectively in molecular simulations (Fig. 2). In addition, chrysomycin A not only inhibited the activity of pure Topo II enzyme but also reduced the expression of Topo II enzyme in cells (Fig. 3B and C). Importantly, chrysomycin A also showed selectivity for cytotoxicity consistent with the literature [39] (Fig. 1B). Topo-II enzyme as a prognostic or predictive marker of chemotherapy sensitivity and clinical outcome of various malignant tumors can guide treatment and medication [74]. Humans encode two isoforms of Topo IIα and IIβ [75]. Topo IIα is an indispensable enzyme that is overexpressed in proliferating cells [75,76]. In contrast to the α isoform, Topo IIβ is expressed in all cell types independent of proliferative status [77]. Therefore, Topo IIα is the best target to avoid adverse side effects such as cardiotoxicity caused by Topo IIβ inhibition. Chrysomycin A belongs to naphthocoumarin glycoside antibiotics (Fig. 1 A), and is a new chemical type of inhibitor of Topo II enzyme reported here, thus broadening the chemical types of antitumor antibiotics that target Topo II enzyme. Nevertheless, since chrysomycin A does induce double-strand breaks (DSBs) in DNA, further examination of the ability or selectivity of chrysomycin A for Topo IIα and IIβ enzymes would be necessary in the future.

Topo II enzyme catalyzes the ATP-dependent cleavage and reconnection of double-stranded DNA [4]. Chrysomycin A inhibits the expression of Topo II enzyme in cells and causes DNA damage. Damaged DNA in cells was assayed by sensor protein γ-H2AX. The results showed that chrysomycin A treatment causes up-regulation of γ-H2AX expression in cells (Fig. 4D), suggesting the occurrence of DNA damage. The accumulation of ROS stimulated by chrysomycin A as a chain reaction also contributes to the biochemical event of DNA damage (Fig. 4 A and B). ROS are recognized as mediators of DNA damage. Recent studies provide mechanistic insights into how ROS affect the cellular response to DNA damage induced by genotoxic treatment in the context of DSBs [78]. Thus, chrysomycin A increased ROS production is associated with the observed induction of DSBs. PARP is a key molecule that senses the pressure of DNA replication [79]. Our data stated that chrysomycin A inhibits the expression of PARP in cells and leads to uncontrolled DNA replication (Fig. 5E and F), resulting in the accumulation of DNA damage mediated by replication pressure. These results firmly indicate that chrysomycin A induces DNA damage in cancer cells. In addition, our results indicated that chrysomycin A acts as a cycle checkpoint (monitoring the operation of DNA mechanisms) abrogator, i.e., arresting the S phase (Fig. 5I and J), and delays cell cycle progression and responds to irreparable DNA damage, thereby inducing ultimately cancer cells apoptosis (Fig. 5 C and D). The Topo II enzyme is cell cycle-dependent and is necessary for the continued excessive division and proliferation of cancer cells [75]. The continued excessive division of cancer cells is strictly regulated by several evolutionarily conserved cell cycle control mechanisms to ensure the production of two genetically identical cells [80]. Although the G2/M phase checkpoint is particularly important in considering the effectiveness of Topo II poisons [81]. However, upon entry into S-phase, Topo II is essential for organizing genome structure, promoting chromosome segregation, and preventing abnormal entry into anaphase and partially inverted sister chromatids [75,82]. Topo IIα levels increase during mid mitotic S phase and decline rapidly after mitotic completion [83]. In addition, Topo II inhibition has been observed in mammalian cells to prevent entry into S-phase (G0) [84,85]. Thus, Topo II activity is regulated in various ways throughout the cell cycle in response to cellular requirements. Our results demonstrate that chrysomycin A treatment impairs the abnormal proliferation of cancer cells (Fig. 5 A and B), and triggers cancer cell apoptosis through DNA damage (Fig. 7). The genetic aberrations and dysregulated signaling pathways of cancer cells allow them to escape apoptosis and proliferate without restriction [1]. Activation of the apoptotic pathway of cancer cells is thus essential for cancer treatment. We confirmed that chrysomycin A treatment triggers cancer cell apoptosis in a caspase 3 activation-dependent manner (Fig. 5H). The remarkable antitumor effect and stable safety of chrysomycin A in vivo were also presented for the first time (Fig. 6). Collectively, the chrysomycin A observed under our experimental conditions had a heavily effective inhibitory effect on the proliferation of transplanted tumors and exhibited excellent safety.

5. Conclusions

In summary, we have established a sophisticated technique to isolate chrysomycin A from marine-derived *Streptomyces*, and importantly demonstrated that chrysomycin A is a new chemical type of Topo II enzyme inhibitor via triggering DNA damage-mediated apoptosis in cancer cells and curbs *KRAS*-mutant lung adenocarcinoma progression in *vivo*. It is not difficult to find that this old drug shows excellent cancer treatment potential. Our data presentation lays the foundation for the

further development of chrysomycin A as a cancer treatment candidate.

CRediT authorship contribution statement

Junmin Zhang, Elaine Lai-Han Leung, and Xiao-Jun Yao are responsible for conceptualization, writing review & editing, and all aspects of the reliability and unbiased interpretation of the data presented and its discussions. Junmin Zhang, Pei Liu, Jianwei Chen, Dahong Yao, Qing Liu, Juanhong Zhang, and Hua-Wei Zhang contribute to the acquisition of data in vitro and in vivo. Xiao-Jun Yao and Liang Liu contribute to administrative, technical, or material support. All authors have read and agreed to the published version of the manuscript.

Conflict of interest

The authors declare that there are no conflicts of interest.

Data Availability

Data will be made available on request.

Acknowledgments

This work was supported by Dr. Neher's Biophysics Laboratory for Innovative Drug Discovery (Grant no. 001/2020/ALC) and the regular grants (File no. 0015/2019/AMJ, 0096/2018/A3, 0114/2020/A3, and 0111/2020/A3) funded by Macao Science and Technology Development Fund, Macau (S.A.R.) China, the 2020 Young Qihuang Scholar award funded by the National Administration of Traditional Chinese Medicine of PRC, the Macao Young Scholars Program (AM201926 and AM2020018), the National Natural Science Foundation of China (82003779 and 82001995), and the Natural Science Foundation of Gansu Province (20JR10RA010).

Appendix A. Supporting information

Supplementary data associated with this article can be found in the online version at doi:10.1016/j.phrs.2022.106565.

References

[1] D. Hanahan, R.A. Weinberg, Hallmarks of cancer: the next generation, Cell 144 (5) (2011) 646–674.
[2] A. Dehshahri, M. Ashrafizadeh, E. Ghasemipour Afshar, A. Pardakhty, A. Mandegary, R. Mohammadinejad, G. Sethi, Topoisomerase inhibitors: Pharmacology and emerging nanoscale delivery systems, Pharmacol. Res 151 (2020), 104551.
[3] K. Hevener, T.A. Verstak, K.E. Lutat, D.L. Riggsbee, J.W. Mooney, Recent developments in topoisomerase-targeted cancer chemotherapy, Acta Pharm. Sin. B 8 (6) (2018) 844–861.
[4] F. Gomez-Herreros, D.N.A. Double, Strand breaks and chromosomal translocations induced by DNA topoisomerase II, Front Mol. Biosci. 6 (2019) 141.
[5] L. Zhang, S. Wang, S. Yin, S. Hong, K.P. Kim, N. Kleckner, Topoisomerase II mediates meiotic crossover interference, Nature 511 (7511) (2014) 551–556.
[6] C. Bailly, Contemporary challenges in the design of topoisomerase II inhibitors for cancer chemotherapy, Chem. Rev. 112 (7) (2012) 3611–3640.
[7] J.L. Nitiss, Targeting DNA topoisomerase II in cancer chemotherapy, Nat. Rev. Cancer 9 (5) (2009) 338–350.
[8] Z. Wang, J. Chen, J. Hu, H. Zhang, F. Xu, W. He, X. Wang, M. Li, W. Lu, G. Zeng, P. Zhou, P. Huang, S. Chen, W. Li, L.P. Xia, X. Xia, cGAS/STING axis mediates a topoisomerase II inhibitor-induced tumor immunogenicity, J. Clin. Invest 129 (11) (2019) 4850–4862.
[9] K. Szlachta, A. Manukyan, H.M. Raimer, S. Singh, A. Salamon, W. Guo, K. S. Lobachev, Y.H. Wang, Topoisomerase II contributes to DNA secondary structure-mediated double-stranded breaks, Nucleic Acids Res. 48 (12) (2020) 6654–6671.
[10] W. Hu, X.S. Huang, J.F. Wu, L. Yang, Y.T. Zheng, Y.M. Shen, Z.Y. Li, X. Li, Discovery of novel topoisomerase II inhibitors by medicinal chemistry approaches, J. Med Chem. 61 (20) (2018) 8947–8980.
[11] P.M. Bruno, M. Lu, K.A. Dennis, H. Inam, C.J. Moore, J. Sheehe, S.J. Elledge, M. T. Hemann, J.R. Pritchard, The primary mechanism of cytotoxicity of the chemotherapeutic agent CX-5461 is topoisomerase II poisoning, Proc. Natl. Acad. Sci. USA 117 (8) (2020) 4053–4060.
[12] Z.Y. Li, G.S. Xu, X. Li, A. Unique, Topoisomerase II inhibitor with dose-affected anticancer mechanisms and less cardiotoxicity, Cells 10 (11) (2021) 3138.
[13] A. Shrestha, S. Park, H.J. Jang, P. Katila, R. Shrestha, Y. Kwon, E.S. Lee, A new phenolic series of indenopyridinone as topoisomerase inhibitors: Design, synthesis, and structure-activity relationships, Bioorg. Med. Chem. 26 (18) (2018) 5212–5223.
[14] M.M. Khalifa, A.A. Al-Karmalawy, E.B. Elkaeed, M.S. Nafie, M.A. Tantawy, I. H. Eissa, H.A. Mahdy, Topo II inhibition and DNA intercalation by new phthalazine-based derivatives as potent anticancer agents: design, synthesis, anti-proliferative, docking, and in vivo studies, J. Enzym. Inhib. Med Chem. 37 (1) (2022) 299–314.
[15] Z. Skok, M. Durcik, D. Gramec Skledar, M. Barancokova, L. Peterlin Masic, T. Tomasic, A. Zega, D. Kikelj, N. Zidar, J. Ilas, Discovery of new ATP-competitive inhibitors of human DNA topoisomerase IIalpha through screening of bacterial topoisomerase inhibitors, Bioorg. Chem. 102 (2020), 104049.
[16] R.L. Siegel, K.D. Miller, H.E. Fuchs, A. Jemal, Cancer Statistics, 2021, 71(1), CA Cancer J. Clin. (2021) 7–33.
[17] C.E. Steuer, M. Behera, V. Ernani, K.A. Higgins, N.F. Saba, D.M. Shin, S. Pakkala, R. N. Pillai, T.K. Owonikoko, W.J. Curran, C.P. Belani, F.R. Khuri, S.S. Ramalingam, Comparison of concurrent use of thoracic radiation with either carboplatin-paclitaxel or cisplatin-etoposide for patients with stage III non-small-cell lung cancer: a systematic review, JAMA Oncol. 3 (8) (2017) 1120–1129.
[18] J.W. Goldman, M. Dvorkin, Y. Chen, N. Reinmuth, K. Hotta, D. Trukhin, G. Statsenko, M.J. Hochmair, M. Ozguroglu, J.H. Ji, M.C. Garassino, O. Voitko, A. Poltoratskiy, S. Ponce, F. Verderame, L. Havel, I. Bondarenko, A. Kazarnowicz, G. Losonczy, N.V. Conev, J. Armstrong, N. Byrne, P. Thiyagarajah, H. Jiang, L. Paz-Ares, C. investigators, Durvalumab, with or without tremelimumab, plus platinum-etoposide versus platinum-etoposide alone in first-line treatment of extensive-stage small-cell lung cancer (CASPIAN): updated results from a randomised, controlled, open-label, phase 3 trial, Lancet Oncol. 22 (1) (2021) 51–65.
[19] S.V. Liu, M. Reck, A.S. Mansfield, T. Mok, A. Scherpereel, N. Reinmuth, M. C. Garassino, J. De Castro Carpeno, R. Califano, M. Nishio, F. Orlandi, J. Alatorre-Alexander, T. Leal, Y. Cheng, J.S. Lee, S. Lam, M. McCleland, Y. Deng, S. Phan, L. Horn, Updated overall survival and PD-L1 subgroup analysis of patients with extensive-stage small-cell lung cancer treated with atezolizumab, carboplatin, and etoposide (IMpower133), J. Clin. Oncol. 39 (6) (2021) 619–630.
[20] C.M. Fillmore, C. Xu, P.T. Desai, J.M. Berry, S.P. Rowbotham, Y.J. Lin, H. Zhang, V. E. Marquez, P.S. Hammerman, K.K. Wong, C.F. Kim, EZH2 inhibition sensitizes BRG1 and EGFR mutant lung tumours to TopoII inhibitors, Nature 520 (7546) (2015) 239–242.
[21] J. Zhang, J. Zhang, Q. Liu, X.X. Fan, E.L. Leung, X.J. Yao, L. Liu, Resistance looms for KRAS G12C inhibitors and rational tackling strategies, Pharmacol. Ther. 229 (2022), 108050.
[22] X.X. Fan, H.D. Pan, Y. Li, R.J. Guo, E.L. Leung, L. Liu, Novel therapeutic strategy for cancer and autoimmune conditions: Modulating cell metabolism and redox capacity, Pharmacol. Ther. 191 (2018) 148–161.
[23] J. Huang, D. Liu, Y. Wang, L. Liu, J. Li, J. Yuan, Z. Jiang, Z. Jiang, W.W. Hsiao, H. Liu, I. Khan, Y. Xie, J. Wu, Y. Xie, Y. Zhang, Y. Fu, J. Liao, W. Wang, H. Lai, A. Shi, J. Cai, L. Luo, R. Li, X. Yao, X. Fan, Q. Wu, Z. Liu, P. Yan, J. Lu, M. Yang, L. Wang, Y. Cao, H. Wei, E.L. Leung, Ginseng polysaccharides alter the gut microbiota and kynurenine/tryptophan ratio, potentiating the antitumour effect of antiprogrammed cell death 1/programmed cell death ligand 1 (anti-PD-1/PD-L1) immunotherapy, Gut 71 (4) (2022) 734–745.
[24] Z.B. Jiang, C. Xu, W. Wang, Y.Z. Zhang, J.M. Huang, Y.J. Xie, Q.Q. Wang, X.X. Fan, X.J. Yao, C. Xie, X.R. Wang, P.Y. Yan, Y.P. Ma, Q.B. Wu, E.L. Leung, Plumbagin suppresses non-small cell lung cancer progression through downregulating ARF1 and by elevating CD8(+) T cells, Pharmacol. Res 169 (2021), 105656.
[25] W.J. Wang, L.F. Mao, H.L. Lai, Y.W. Wang, Z.B. Jiang, W. Li, J.M. Huang, Y.J. Xie, C. Xu, P. Liu, Y.M. Li, E.L.H. Leung, X.J. Yao, Dolutegravir derivative inhibits proliferation and induces apoptosis of non-small cell lung cancer cells via calcium signaling pathway, Pharmacol. Res. 161 (2020), 105129.
[26] E.L. Leung, L.X. Luo, Y. Li, Z.Q. Liu, L.L. Li, D.F. Shi, Y. Xie, M. Huang, L.L. Lu, F. G. Duan, J.M. Huang, X.X. Fan, Z.W. Yuan, J. Ding, X.J. Yao, D.C. Ward, L. Liu, Identification of a new inhibitor of KRAS-PDEdelta interaction targeting KRAS mutant nonsmall cell lung cancer, Int J. Cancer 145 (5) (2019) 1334–1345.
[27] C. Wei, X. Yao, Z. Jiang, Y. Wang, D. Zhang, X. Chen, X. Fan, C. Xie, J. Cheng, J. Fu, E.L. Leung, Cordycepin inhibits drug-resistance non-small cell lung cancer progression by activating AMPK signaling pathway, Pharm. Res 144 (2019) 79–89.
[28] A.G. Atanasov, S.B. Zotchev, V.M. Dirsch, T. International natural product sciences, C.T. Supuran, natural products in drug discovery: advances and opportunities, Nat. Rev. Drug Discov. 20 (3) (2021) 200–216.
[29] A. Kornienko, A. Evidente, M. Vurro, V. Mathieu, A. Cimmino, M. Evidente, W. A. van Otterlo, R. Dasari, F. Lefranc, R. Kiss, Toward a cancer drug of fungal origin, Med. Res Rev. 35 (5) (2015) 937–967.
[30] J. Lin, D. Zhou, T.A. Steitz, Y.S. Polikanov, M.G. Gagnon, Ribosome-targeting antibiotics: modes of action, mechanisms of resistance, and implications for drug design, Annu Rev. Biochem 87 (2018) 451–478.
[31] C.D. Mohan, S. Rangappa, S.C. Nayak, R. Jadimurthy, L. Wang, G. Sethi, M. Garg, K.S. Rangappa, Bacteria as a treasure house of secondary metabolites with anticancer potential, Semin Cancer Biol. 86 (Pt 2) (2021) 998–1013.
[32] F. Strelitz, H. Flon, I.N. Asheshov, Chrysomycin: a new antibiotic substance for bacterial viruses, J. Bacteriol. 69 (3) (1955) 280–283.
[33] I. Sava, D. Mirodescu-Greceanu, O. Lutescu, Chrysomycin in suppurative surgical and gynecological disorders, Bul. Stiint. Sect. Stiint. Med. Acad. Repub. Pop. Rom. 6 (1) (1954) 131–165.

[34] J.A. Matson, W.C. Rose, J.A. Bush, R. Myllymaki, W.T. Bradner, T.W. Doyle, Antitumor activity of chrysomycins M and V, J. Antibiot. 42 (9) (1989) 1446–1448.
[35] U. Weiss, K. Yoshihira, R.J. Highet, R.J. White, T.T. Wei, The chemistry of the antibiotics chrysomycin A and B. Antitumor activity of chrysomycin A, J. Antibiot. 35 (9) (1982) 1194–1201.
[36] M.K. Kudinova, V.V. Kuliaeva, N.P. Potapova, L.M. Rubasheva, T.S. Maksimova, Separation and characteristics of the components of the antibiotic virenomycin, Antibiotiki 27 (7) (1982) 507–511.
[37] M.G. Brazhnikova, M.K. Kudinova, V.V. Kuliaeva, N.P. Potapova, L.M. Rubasheva, Structure of the antibiotic virenomycin, Antibiotiki 29 (12) (1984) 884–892.
[38] S.K. Jain, A.S. Pathania, R. Parshad, C. Raina, A. Ali, A.P. Gupta, M. Kushwaha, S. Aravinda, S. Bhushan, S.B. Bharate, R.A. Vishwakarma, Chrysomycins A–C, antileukemic naphthocoumarins from Streptomyces sporoverrucosus, RSC Adv. 3 (43) (2013) 21046–21053.
[39] B. Muralikrishnan, V.M. Dan, J.S. Vinodh, V. Jamsheena, R. Ramachandran, S. Thomas, S.G. Dastager, K.S. Kumar, R.S. Lankalapalli, R.A. Kumar, Antimicrobial activity of chrysomycin A produced by Streptomyces sp. against Mycobacterium tuberculosis, RSC Adv. 7 (58) (2017) 36335–36339.
[40] F. Wu, J. Zhang, F. Song, S. Wang, H. Guo, Q. Wei, H. Dai, X. Chen, X. Xia, X. Liu, L. Zhang, J.Q. Yu, X. Lei, Chrysomycin A derivatives for the treatment of multidrug-resistant tuberculosis, ACS Cent. Sci. 6 (6) (2020) 928–938.
[41] D. Trauner, C. Fischer, Chrysomycin A and derivatives against multi-drug-resistant tuberculosis, Synfacts 16 (08) (2020) 0986.
[42] B. Muralikrishnan, L.K. Edison, A. Dusthackeer, G.R. Jijimole, R. Ramachandran, A. Madhavan, R.A. Kumar, Chrysomycin A inhibits the topoisomerase I of Mycobacterium tuberculosis, J. Antibiot. 75 (4) (2022) 226–235.
[43] M. Liu, S.S. Zhang, D.N. Liu, Y.L. Yang, Y.H. Wang, G.H. Du, Chrysomycin A attenuates neuroinflammation by down-regulating NLRP3/cleaved caspase-1 signaling pathway in LPS-stimulated mice and BV2 cells, Int J. Mol. Sci. 22 (13) (2021).
[44] K. Chen, F. Wu, X. Lei, Function-oriented natural product synthesis, Chin. J. Chem. 39 (4) (2021) 838–854.
[45] W. Liu, B. Hong, J. Wang, X. Lei, New strategies in the efficient total syntheses of polycyclic natural products, Acc. Chem. Res 53 (11) (2020) 2569–2586.
[46] H.J. Ni, S.Y. Lv, Y.T. Sheng, H. Wang, X.H. Chu, H.W. Zhang, Optimization of fermentation conditions and medium compositions for the production of chrysomycin a by a marine-derived strain Streptomyces sp. 891, Prep. Biochem. Biotechnol. 51 (10) (2021) 998–1003.
[47] X. Hu, Y. Tang, Y. Liu, X. Pei, Z. Huang, F. Song, H. Zhang, Comprehensive genomic analysis of marine strain Streptomyces sp. 891, an excellent producer of chrysomycin A with therapeutic potential, Mar. Drugs 20 (5) (2022).
[48] R.A. Friesner, J.L. Banks, R.B. Murphy, T.A. Halgren, J.J. Klicic, D.T. Mainz, M. P. Repasky, E.H. Knoll, M. Shelley, J.K. Perry, D.E. Shaw, P. Francis, P.S. Shenkin, Glide: a new approach for rapid, accurate docking and scoring. 1. Method and assessment of docking accuracy, J. Med Chem. 47 (7) (2004) 1739–1749.
[49] R.A. Friesner, R.B. Murphy, M.P. Repasky, L.L. Frye, J.R. Greenwood, T.A. Halgren, P.C. Sanschagrin, D.T. Mainz, Extra precision glide: docking and scoring incorporating a model of hydrophobic enclosure for protein-ligand complexes, J. Med. Chem. 49 (21) (2006) 6177–6196.
[50] T.B. Thapa Magar, S. Hee Seo, A. Shrestha, J.A. Kim, S. Kunwar, G. Bist, Y. Kwon, E.S. Lee, Synthesis and structure-activity relationships of hydroxylated and halogenated 2,4-diaryl benzofuro[3,2-b]pyridin-7-ols as selective topoisomerase IIalpha inhibitors, Bioorg. Chem. 111 (2021), 104884.
[51] R. Ishida, T. Miki, T. Narita, R. Yui, M. Sato, K.R. Utsumi, K. Tanabe, T. Andoh, Inhibition of intracellular topoisomerase-Ii by antitumor Bis(2,6-Dioxopiperazine) derivatives - mode of cell-growth inhibition distinct from that of cleavable complex-forming type inhibitors, Cancer Res. 51 (18) (1991) 4909–4916.
[52] A. Herrero-Ruiz, P.M. Martinez-Garcia, J. Terron-Bautista, G. Millan-Zambrano, J. A. Lieberman, S. Jimeno-Gonzalez, F. Cortes-Ledesma, Topoisomerase IIalpha represses transcription by enforcing promoter-proximal pausing, Cell Rep. 35 (2) (2021), 108977.
[53] C.M. Chien, J.C. Yang, P.H. Wu, C.Y. Wu, G.Y. Chen, Y.C. Wu, C.K. Chou, C. H. Tseng, Y.L. Chen, L.F. Wang, C.C. Chiu, Phytochemical naphtho[1,2-b] furan-4,5dione induced topoisomerase II-mediated DNA damage response in human non-small-cell lung cancer, Phytomedicine 54 (2019) 109–119.
[54] E.L.H. Leung, L.X. Luo, Z.Q. Liu, V.K.W. Wong, L.L. Lu, Y. Xie, N. Zhang, Y.Q. Qu, X.X. Fan, Y. Li, M. Huang, D.K. Xiao, J. Huang, Y.L. Zhou, J.X. He, J. Ding, X.J. Yao, D.C. Ward, L. Liu, Inhibition of KRAS-dependent lung cancer cell growth by deltarasin: blockage of autophagy increases its cytotoxicity, Cell Death Dis. 9 (2) (2018) 216.
[55] Z.L. Song, J. Zhang, Q. Xu, D. Shi, X. Yao, J. Fang, Structural modification of aminophenylarsenoxides generates candidates for leukemia treatment via thioredoxin reductase inhibition, J. Med. Chem. 64 (21) (2021) 16132–16146.
[56] J. Zhang, Z.Q. Zheng, Q. Xu, Y. Li, K. Gao, J. Fang, Onopordopicrin from the new genus Shangwua as a novel thioredoxin reductase inhibitor to induce oxidative stress-mediated tumor cell apoptosis, J. Enzym. Inhib. Med. Chem. 36 (1) (2021) 790–801.
[57] V.A. Stonik, T.N. Makarieva, L.K. Shubina, Antibiotics from marine bacteria, Biochemistry 85 (11) (2020) 1362–1373.
[58] C. Xie, Y. Li, L.L. Li, X.X. Fan, Y.W. Wang, C.L. Wei, L. Liu, E.L. Leung, X.J. Yao, Identification of a new potent inhibitor targeting KRAS in non-small cell lung cancer cells, Front Pharm. 8 (2017) 823.
[59] F.P. Gasparro, R.M. Knobler, R.L. Edelson, The effects of gilvocarcin V and ultraviolet radiation on pBR322 DNA and lymphocytes, Chem. Biol. Inter. 67 (3–4) (1988) 255–265.
[60] W. Zhang, P. Gou, J.M. Dupret, C. Chomienne, F. Rodrigues-Lima, Etoposide, an anticancer drug involved in therapy-related secondary leukemia: Enzymes at play, Transl. Oncol. 14 (10) (2021), 101169.
[61] E. Karatas, E. Foto, T. Ertan-Bolelli, G. Yalcin-Ozkat, S. Yilmaz, S. Ataei, F. Zilifdar, I. Yildiz, Discovery of 5-(or 6)-benzoxazoles and oxazolo[4,5-b]pyridines as novel candidate antitumor agents targeting hTopo IIalpha, Bioorg. Chem. 112 (2021), 104913.
[62] B. Kapron, A. Plazinska, W. Plazinski, T. Plech, Identification of the first-in-class dual inhibitors of human DNA topoisomerase IIalpha and indoleamine-2,3-dioxygenase 1 (IDO 1) with strong anticancer properties, J. Enzym. Inhib. Med. Chem. 38 (1) (2023) 192–202.
[63] X. Pan, T.Y. Mao, Y.W. Mai, C.C. Liang, W.H. Huang, Y. Rao, Z.S. Huang, S. L. Huang, Discovery of quinacrine as a potent topo II and Hsp90 dual-target inhibitor, repurposing for cancer therapy, Molecules 27 (17) (2022).
[64] A. Mojumdar, J. Deka, Assaying the activity of helicases, in: R. Tuteja (Ed.), Helicases from All Domains of Life, Academic Press, 2019, pp. 235–246.
[65] J.L. Nitiss, K. Kiianitsa, Y. Sun, K.C. Nitiss, N. Maizels, Topoisomerase assays, Curr. Protoc. 1 (10) (2021), e250.
[66] J. Zhang, D. Duan, Z.L. Song, T. Liu, Y. Hou, J. Fang, Small molecules regulating reactive oxygen species homeostasis for cancer therapy, Med Res Rev. 41 (1) (2021) 342–394.
[67] R.M. Chabanon, M. Rouanne, C.J. Lord, J.C. Soria, P. Pasero, S. Postel-Vinay, Targeting the DNA damage response in immuno-oncology: developments and opportunities, Nat. Rev. Cancer 21 (11) (2021) 701–717.
[68] B.A. Carneiro, W.S. El-Deiry, Targeting apoptosis in cancer therapy, Nat. Rev. Clin. Oncol. 17 (7) (2020) 395–417.
[69] A.R. Moore, S.C. Rosenberg, F. McCormick, S. Malek, RAS-targeted therapies: is the undruggable drugged? Nat. Rev. Drug Disco 19 (8) (2020) 533–552.
[70] M.A.M. Reijns, D.A. Parry, T.C. Williams, F. Nadeu, R.L. Hindshaw, D.O. Rios Szwed, M.D. Nicholson, P. Carroll, S. Boyle, R. Royo, A.J. Cornish, H. Xiang, K. Ridout, C. Genomics England Research, G.P. Colorectal Cancer Domain Uk, A. Schuh, K. Aden, C. Palles, E. Campo, T. Stankovic, M.S. Taylor, A.P. Jackson, Signatures of TOP1 transcription-associated mutagenesis in cancer and germline, Nature 602 (7898) (2022) 623–631.
[71] A. Thomas, C.E. Redon, L. Sciuto, E. Padiernos, J. Ji, M.J. Lee, A. Yuno, S. Lee, Y. Zhang, L. Tran, W. Yutzy, A. Rajan, U. Guha, H. Chen, R. Hassan, C.C. Alewine, E. Szabo, S.E. Bates, R.J. Kinders, S.M. Steinberg, J.H. Doroshow, M.I. Aladjem, J. B. Trepel, Y. Pommier, Phase I study of ATR inhibitor M6620 in combination with topotecan in patients with advanced solid tumors, J. Clin. Oncol. 36 (16) (2018) 1594–1602.
[72] A. Vanden Broeck, C. Lotz, R. Drillien, L. Haas, C. Bedez, V. Lamour, Structural basis for allosteric regulation of Human Topoisomerase IIalpha, Nat. Commun. 12 (1) (2021) 2962.
[73] M.K. Kharel, P. Pahari, M.D. Shepherd, N. Tibrewal, S.E. Nybo, K.A. Shaaban, J. Rohr, Angucyclines: biosynthesis, mode-of-action, new natural products, and synthesis, Nat. Prod. Rep. 29 (2) (2012) 264–325.
[74] M. Nair, S.S. Sandhu, A.K. Sharma, Cancer molecular markers: a guide to cancer detection and management, Semin Cancer Biol. 52 (Pt 1) (2018) 39–55.
[75] J.H. Lee, J.M. Berger, Cell cycle-dependent control and roles of DNA topoisomerase II, Genes 10 (11) (2019) 859.
[76] Y. Pommier, Y. Sun, S.N. Huang, J.L. Nitiss, Roles of eukaryotic topoisomerases in transcription, replication and genomic stability, Nat. Rev. Mol. Cell Biol. 17 (11) (2016) 703–721.
[77] M.I. Sandri, D. Hochhauser, P. Ayton, R.C. Camplejohn, R. Whitehouse, H. Turley, K. Gatter, I.D. Hickson, A.L. Harris, Differential expression of the topoisomerase II alpha and beta genes in human breast cancers, Br. J. Cancer 73 (12) (1996) 1518–1524.
[78] U.S. Srinivas, B.W.Q. Tan, B.A. Vellayappan, A.D. Jeyasekharan, ROS and the DNA damage response in cancer, Redox Biol. 25 (2019), 101084.
[79] A. Maya-Mendoza, P. Moudry, J.M. Merchut-Maya, M. Lee, R. Strauss, J. Bartek, High speed of fork progression induces DNA replication stress and genomic instability, Nature 559 (7713) (2018) 279–284.
[80] H.K. Matthews, C. Bertoli, R.A.M. de Bruin, Cell cycle control in cancer, Nat. Rev. Mol. Cell Biol. 23 (1) (2022) 74–88.
[81] D.A.N., B. Gabrielli, Topoisomerase II inhibitors and poisons, and the influence of cell cycle checkpoints, Curr. Med Chem. 24 (15) (2017) 1504–1519.
[82] T. Uemura, H. Ohkura, Y. Adachi, K. Morino, K. Shiozaki, M. Yanagida, DNA topoisomerase II is required for condensation and separation of mitotic chromosomes in S. pombe, Cell 50 (6) (1987) 917–925.
[83] M.M. Heck, W.N. Hittelman, W.C. Earnshaw, Differential expression of DNA topoisomerases I and II during the eukaryotic cell cycle, Proc. Natl. Acad. Sci. USA 85 (4) (1988) 1086–1090.
[84] M.S. Hossain, N. Akimitsu, T. Takaki, H. Hirai, K. Sekimizu, ICRF-193, a catalytic inhibitor of DNA topoisomerase II, inhibits re-entry into the cell division cycle from quiescent state in mammalian cells, Genes Cells 7 (3) (2002) 285–294.
[85] M.S. Hossain, K. Kurokawa, N. Akimitsu, K. Sekimizu, DNA topoisomerase II is required for the G0-to-S phase transition in Drosophila Schneider cells, but not in yeast, Genes Cells 9 (10) (2004) 905–917.